

FAN ZHUANGQING
LI JUNCHENG
LI HUIMIN
LU YONGGANG
WANG JIANMIN
CHEN JING
and
KANG JIANYI

Theoretical analysis and numerical simulation of detonation-driven directional dispersing of metal particles

In order to achieve directional dispersing of metal particles, a detonation-driven model placing metal particles and explosives together inside a rigid pipe was developed in this study. The one-dimensional detonation wave theoretical analysis was conducted to explore the relationship between the dispersing velocity and the mass of particles and explosives. Moreover, the three-dimensional finite element simulations were performed with mass ratio of explosive/particle at 0.5:1, 1:1 and 2:1 respectively, while the particle diameter was 0.05cm. An empirical formula describing the relationship between the dispersing velocity and the mass ratio of explosive particle was obtained as the result of theoretical analysis. The simulation results demonstrated that the particles fly along the axis steadily, with little scattering and good directionality. The dispersing velocities derived from theoretical analysis were found to agree with the results of the numerical simulations, which suggested the availability of this investigation.

Key Words: Detonation-driven, particle, directional dispersing, theoretical analysis, numerical simulation

1. Introduction

It has been extensively applied in the military domain that pushing objects of a certain mass movement at high velocity by using explosive energy[1], such as shooting of various types of rifles, fuel sprinkling of fuel-air explosive, metal powder dispersing of low collateral damage ammunition [2] and so on. In recent years, explosive-driven metal particles dispersing become a new concern because the individual particle is small in size and light in weight which contributes to rapid velocity attenuation and therefore the dispersing

radius of a particle could be effectively controlled by altering the mass of the particles and the explosives. The previous researches mainly focused on the momentum transfer and heat transmit during shock interaction with metal particles [3-6]. The numerical simulation explained the detonation wave propagation of explosive charges containing metal particles [7, 8].

The structure that particles surrounded the centered explosive was generally adopted in the aforementioned experiments. However, this kind of structure also has such limitations as large quantity of explosive, poor repetitiveness, long period of preparation for experiment, uncontrollable dispersing direction of particles and inconvenience of velocity measurement because of the random scattering of particles. In the simulation analysis of detonation-driven particle dispersing, only single particle was included in computational model. Thus, there is currently limited understanding about the behaviour of particle flow produced by detonation-driven dispersing of large amount of metal particles.

This paper developed a detonation-driven model placing metal particles and explosives together inside a rigid pipe which charged just small quantity of explosives. Then one-dimensional theoretical analysis and three-dimensional finite element simulation were conducted to characterize the detonation-driven directional dispersing of metal particles. The dispersing velocity of particles under different mass ratio of explosives/particles would be discussed.

2. One-dimensional explosion dispersing theoretical model

A one-dimensional explosion dispersing model was initially developed to explore the extreme dispersing velocity under a certain quantity of explosive, and to find the relationship between the dispersing velocity and the mass ratio of explosives/particles. As illustrated in Fig.1, suppose the section area of the rigid cylindrical barrel (hereinafter referred to as barrel) is A , and its length is infinite; the interior

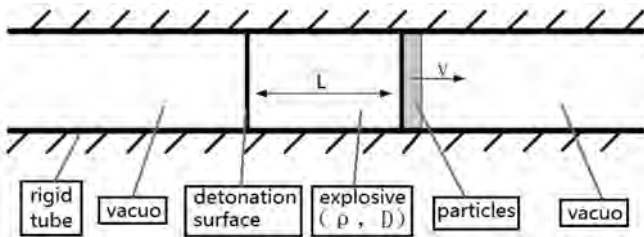
Messrs. Fan Zhuangqing, Wang Jianmin, Chen Jing and Kang Jianyi, State Key Laboratory of Trauma, Burns and Combined Injury, Institute of Surgery, Third Military Medical University, Chongqing 40042 and Li Juncheng, Li Huimin and Lu Yonggang, Institute of Systems of Engineering, China Academy of Engineering Physics, Mianyang 621 900, Sichuan, China

explosive placing density is ρ , the explosion velocity is D , and the length is L ; the right side is placed with M particle group with total mass M , it is completely considered as a cylinder, and the particle group is moving completely upon explosion; the left end of explosive is ignited, it is considered as coordinate $X=0$ point. In order to simplify it, the other areas in the barrel are all vacuums.

After igniting the explosive, the detonation wave form is a gleam of central simple wave spreading toward the right, and could be described as the formula (1) below with one-dimensional isentropy in constant flowing basic formula special solution:

$$\begin{cases} x = (u + c)t \\ u = c - \frac{D}{2} \end{cases} \quad \dots \quad (1)$$

when $t = L/D$, the detonation waves reach the particle groups, the first reflection compressive waves reflected from the surfaces of particle groups start to spread toward the left detonation products, meanwhile, because the particle groups are functioned by the detonation products, they start to move toward right, each of the subsequent rightward wave continuously catches up and functions on the particle group, at the same time a series of leftward waves are reflected [9].



where c_b is the sound velocity at the particle group surface, and it obtains the following after applying formula (3) into formula (2):

$$\frac{dv}{dt} = \frac{16}{27} \frac{A\rho}{MD} c_b^3 = \frac{\eta c_b^3}{LD} \quad \dots \quad (5)$$

where $\eta = \frac{16}{27} \frac{m}{M}$

Each rightward wave is spreading at its own $(u+c)$ velocity, and this value remains unchanged alongside the featured direction of the wave [10], if it encounters the moving part

TABLE 1: COMPUTING VELOCITIES IN DIFFERENT MASS RATIOS

Explosive mass, m (g)	Explosive length, L (cm)	Dispersal mass, M (g)	Diameter of rigid pipe (cm)	Mass ratio of explosive/particle	Computing velocity, m/s
3.4	0.66	6.8	2	0.5:1	802.62
6.8	1.33	6.8	2	1:1	1337.31
13.6	2.66	6.8	2	2:1	2042.59

TABLE 2: OPERATING CONDITIONS OF NUMERICAL SIMULATION

Model no.	Mass of explosive m(g)	Explosive length L (cm)	Mass of particles, M(g)	Mass ratio of explosive /particle	Thickness of particle layer (cm)	Diameter of rigid pipe (cm)	Total length of rigid pipe (cm)
1	3.4	0.66	6.8	0.5:1	0.15	2	13
2	6.8	1.33	6.8	1:1	0.15	2	13
3	13.6	2.66	6.8	2:1	0.15	2	13

obtain the velocity of the particle group:

$$v = D \left[1 + \frac{\theta - 1}{\eta\theta} - \frac{L\theta}{Dt} \right] \quad \dots (13)$$

According to the deduce above, if t tends to be infinite $\theta = \frac{1}{\sqrt{1+2\eta}}$, apply this formula into formula (13), to obtain the extreme velocity of the particle group:

$$v_{max} = D \left[1 + \frac{1}{\eta} - \frac{\sqrt{1+2\eta}}{\eta} \right] \quad \dots (14)$$

According to formula (14), when the explosive type is TNT and density is 1.63 g/cm^3 , the explosion velocity is 6930 m/s , the rigid cylindrical diameter is 2 cm , the particle group mass is 6.8 g , and when the density is 14.5 g/cm^3 , the calculation results of particle extreme dispersing velocity under conditions of different explosive/metallic particle mass ratios are listed in the Table 1.

3. Three-dimensional finite element simulation

3.1 MODELLING

The explicit dynamic analysis software ANSYS/LS-DYNA was used to establish the finite element model, with model structure as illustrated in Fig.2. The model consists of four parts: that is the rigid barrel with one end open, air, explosive and the tungsten powder layer composed of particle groups.

The finite element models in three operating conditions are established according to different explosive charge, and

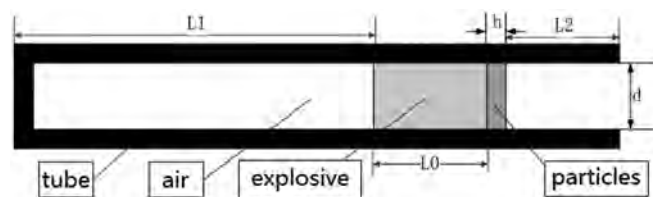


Fig.2 Schematic diagram of finite element model structure

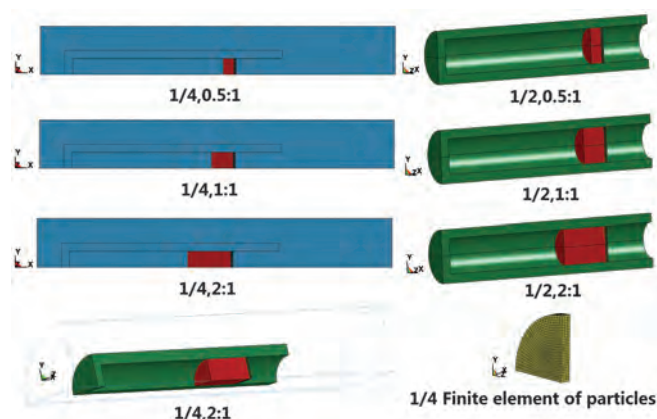


Fig.3 Finite element model diagram

refer to Table 2 for parameters.

The finite element model established is as indicated in Fig.3. Considering the symmetry of the entire model structure, 1/4 model is established to save the calculation costs, the TNT explosive is adopted in the model, the tungsten particles are adopted as powder particles, with mass of 6.8g , totally 7056 particles, and all the maximum feature size of the particles is $500\mu\text{m}$.

All models' element type is solid 164, and all meshes are 8-node hexahedral grids. The explosive and air are adopted with co-node EULER grid descriptions, and multi-material ALE algorithm. The barrel and tungsten particles are adopted with LAGRANGE algorithm. The fluid-structure coupling algorithm is adopted for control of the fluid units composed of explosive and air and the solid units composed of barrel particles, so as to simulate the driving effect from the explosive on tungsten particles. The model symmetric surfaces are defined as symmetric binding, transmission binding is applied on surrounding of the air field, so as to avoid the impact waves from reflecting on boundary of air field and causing computing errors. The unit system adopted for the model is $\text{cm-g-}\mu\text{s}$, and the ignition manner is set as explosive bottom

plane ignition. Due to the explosive mass in model 1 is small, the calculation duration is 200 μ s, and the calculation duration for model 2 and 3 is 120 μ s. The overall particle layer modeling and node failure method were adopted to reduce the element amount and to improve the matching between the particle mesh and the integrated model.

3.2 MATERIAL MODELS AND PARAMETERS

The air is described with NULL material model and the linear polynomial equation complying with the gamma law:

$$P = (\gamma - 1)\rho e \quad \dots \quad (15)$$

In this formula r is density, e is energy within ratio, and g is polytrophic indices. Refer to Table 3 for parameters of the air state equation:

TABLE 3: MATERIAL PARAMETERS OF AIR

$\rho/(g \cdot cm^{-3})$	$e/(MJ \cdot kg^{-1})$	g
1.293	2.00	140

TABLE 4: MATERIAL PARAMETERS OF EXPLOSIVE

Density $\rho/(g \cdot cm^{-3})$	Explosion velocity $D/(m \cdot s^{-1})$	A	B	R_1	R_2	w	$e/(kJ \cdot g^{-1})$
1.63	6025	3.74	0.073	4.15	0.95	0.30	4.19

The explosive is described with JWL state

$$P = A \left(1 - \frac{\omega \eta}{R_1} \right) e^{-R_1/\eta} + B \left(1 - \frac{\omega \eta}{R_2} \right) e^{-R_2/\eta} + \omega \eta \rho_0 e \quad \dots \quad (16)$$

In this formula, e is the internal energy of unit mass, r_0 is the initial density of the explosive, r is density of the detonation products, and $\eta = \rho/\rho_0$, A , B , w , R_1 , R_2 are constants (Table 4).

Iron or steel materials are adopted for rigid barrels, with density of 7.8 g/cm³, use *MAT_RIGID material model to describe, and restrict its displacement and rotation:

Employ the follow-up hardened material model PLASTIC_KINEMATIC with varying items for the particle groups, in order to avoid from being deleted when the particle material unit reaches the invalid strength in calculation, the yield strength s_0 of the particle shall be set with a bigger value, and refer to Table 5 for the specific material parameters.

3.3 CONTACTING AND FAILURE MODE

The fluid-structure interaction algorithm *CONSTRAINED_LAGRANGE_IN_SOLID is adopted

TABLE 5: PARAMETERS OF METAL PARTICLE

r (kg/m ³)	E	u	s_0 /MPA	b
14.5	3.15	0.28	1300	1.0

between the explosive air and the barrel particle groups, and the mutual collisions might occur between particles, and it is defined as the self-contacting *CONTACT_AUTOMATIC_SINGLE_SURFACE, and between the particle and barrel is defined as automatic surface contact *CONTACT_AUTOMATIC_SURFACE_TO_SURFACE.

Because there are huge amount of particles, if the spherical particles are established, then the single particle diameter is 500 μ m, and the single grid dimension is too small after classifying grids, and it is unmatched with the overall grid dimensions, and the grid data is huge, as a result, it is impossible to calculate. Therefore, the particle groups are completely modelled, with each layer thickness of 500 μ m, classify it as a cubic grid, with the maximum feature size 500 μ m, define the grids as node invalid binding *CONSTRAINED_TIED_NODES_FAILURE, and define the invalid stress as 0.5 Mpa, when the detonation waves and detonation products reach the particle layers, the particle groups will disperse toward the port driven by the detonation.

The tungsten particles with total mass 6.8 g, the particle density 16.5g/cm³, use this method to establish 7056 particles totally, and it shall be 7168 particles if spherical particles are established, with difference less than 1.5%. If the spherical particles are divided into grids, then there will be 16 portions a diameter direction, and there will be 2048 portions of single particle grids, the minimum size of the grid is 3.125 μ m; if the overall modelling as this article is adopted, one grid is required for the single particle, with the minimum feature size of 500 μ m, not only the quantity of grids is greatly cut down, but also the matching degree between the grids and the overall grids is significantly increased.

4. Results and analysis of numerical simulation

4.1 DISPERSING OF METAL PARTICLES

After calculations, the particle groups “gush out” from the barrel port alongside the barrel direction after ignition of the explosive under function from the detonation-driving, and continuously fly ahead in the air. Fig.4 indicates the dispersing shapes of particle clusters with three explosive charge upon completion of the calculation.

4.2 DETONATION-DRIVEN PROCESS

The detonation-driven particle group processes under different quantity of explosive charges are almost the same. Take the mass ratio of explosive/particle 2:1 as an example, and analyze the whole process of detonation-driven process.

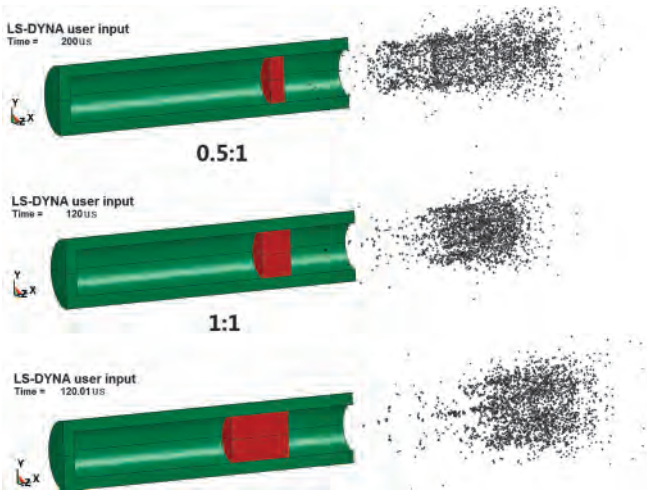


Fig.4 Dispersing of metal particles under different mass ratio of explosive/particle

Fig.5 shows the pressure distribution during detonation-driven processes at different time.

At the initial moment, the end surface established has plane ignition, with rightward spreading plane detonation waves formed. In Fig.5a, when $t = 2\mu s$, the plane waves start to spread rightward. In Fig.5b, $t = 4\mu s$, the detonation waves reach the surfaces of particle layer, the binding between particles will be invalid. At the moment $t = 8\mu s$, the particle layers in Fig.5c have scattered, the self-contact is set to prevent from the “mutual penetration” phenomenon between particles, and the particle groups disperse to the port under effect from the detonation products and impact waves. When $t = 22\mu s$, in Fig.5d, the expansion waves spreading from port to left start to function on the particle groups, and the “disordered dispersing” phenomenon starts to appear in the complicated flow field with mingling of detonation products and expansion waves, the particles close to the barrel wall are

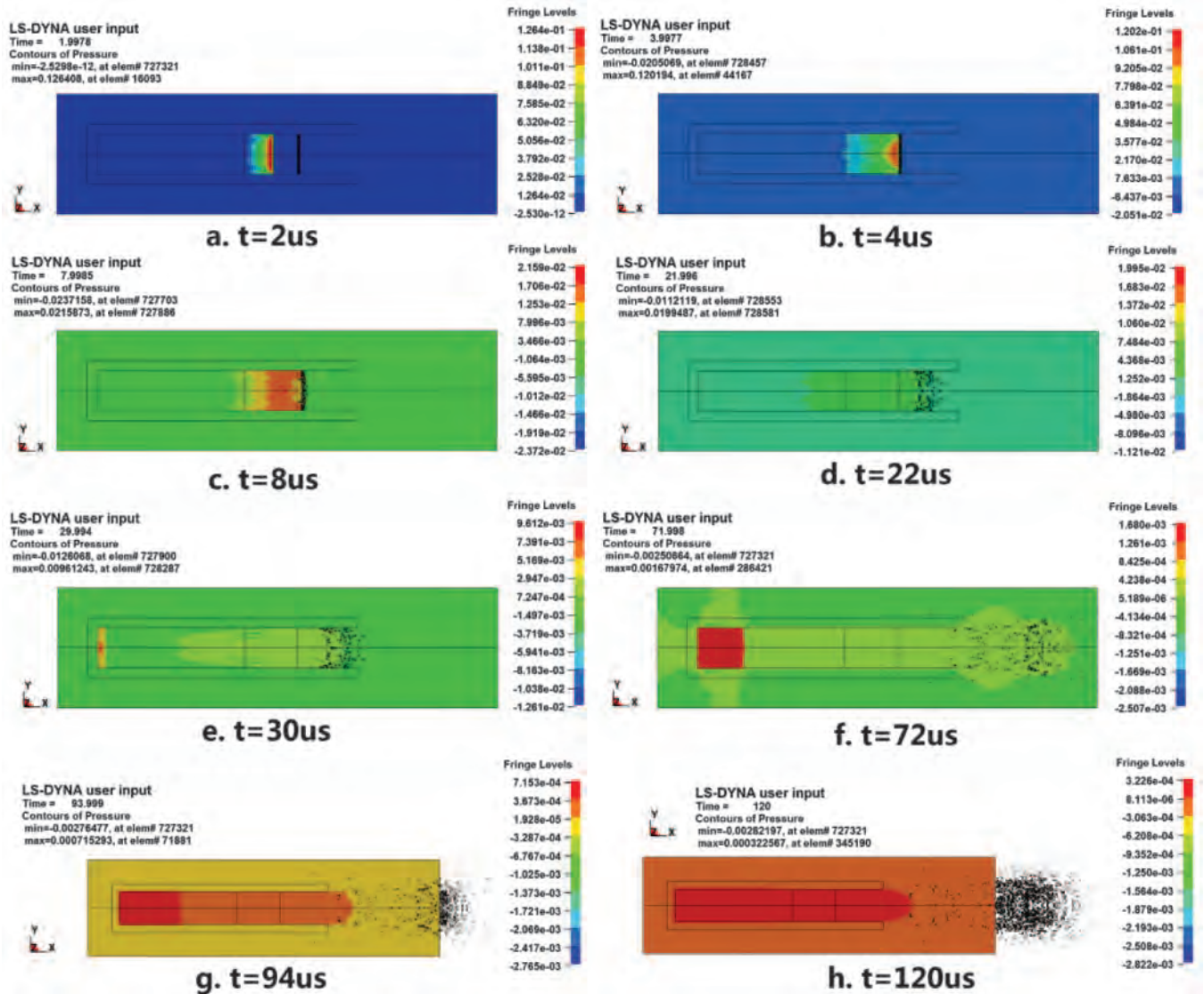


Fig.5 Pressure distributions during explosion driving process

in collision with the barrel wall, as a result, the particles change their direction and reduce their velocity, which aggravates the “disordered dispersing” phenomenon. When $t = 30\mu s$, the front particles in Fig.5(e) fly out from the port, the particles close to barrel wall are continuously colliding with the barrel wall under effect from the swelling of detonation products, the complicated flow field at the port makes the particle groups to “elongate the dispersing”; the detonation products dispersing and spreading leftward after ignition and the impact waves successively arrive at the bottom end of the barrel, and they are continuously gathered and overlapped at the barrel bottom, as a result, the bottom pressure of the barrel is increased. When $t = 72\mu s$, most particle groups in Fig.5f have flown out from the port, the high pressure area at the barrel bottom are also continuously increased, the detonation products at the port are “gushed” out from the port together with the particles, and they are consecutively functioning on the particles to accelerate their flying. In Fig.5g when $t = 94\mu s$, the impact waves gathered at the bottom spread toward the port after reflecting with the detonation products, the pressure inside the barrel is positive, the areas besides the port are mostly negative pressure, and the particles are flying in the air. Due to restrictions from the modeling dimensions, the length of the area field is limited, in Fig.5h when $t = 120\mu s$, most of the particle clusters have flown out from the established area field, and are flying stably.

In a word, the dispersing process from the detonation-driven particle cluster is divided into four stages: (1) Explosive ignition, the particle clusters start to scatter under the plane waves, and the clustered particles start to increase velocity completely; (2) Under comprehensive effect from the detonation products and the expansion waves, the particles are colliding the barrel walls, the velocity of some particles is lower than the overall velocity, and it is generally in a “disordered elongated shape” and flying out of the port with accelerated velocity; (3) The pre-segment of the particle clusters fly out from the port, the complicated flow fields at the port continuously lengthen the scattering of the particle clusters, and the impact waves and detonation products gather and reflect at the bottom of the barrel; (4) The detonation products will not function on particles, the particles enter into air and fly, and scatter under air resistance, it is positive area inside the barrel and the others are negative pressure.

4.3 PARTICLE FLYING VELOCITY

Fig.6 indicates the average velocity values of particle clusters and the velocity process curves of the chosen particle points with three explosive charge. The left picture indicates the overall average velocity of the particle groups, and the right picture indicates the particles with the maximum velocity and its typical particles.

The above velocity process curves indicate (1) The overall average velocity of the particle groups start to stabilize after reaching $80\mu s$, at this moment the particles have flown out of the port, the detonation products will not function on the particles; (2) With increase of the explosive charge, the overall velocity from the particle groups and the maximum velocity from the single particle are remarkably increased, and the acceleration duration is prolonged. Table 6 compares the value simulated results of the particle velocity and the theoretical values as below:

When the explosive/particle mass ratio is 0.5 and 1, the difference between the simulated velocity and theoretical velocity is below 15%, which indicates the value simulation perfectly matches with the theoretical analyses on forecasting the maximum velocity of the particles; with increase of the explosive charge, the velocity acceleration of value simulation is not in a linear acceleration, the difference from the theoretical value starts to increase, in addition, the average velocity of value simulation is below the maximum theoretical velocity, the possible reasons: (1) The theoretical model is under the hypothesis with an indefinitely long rigid barrel under vacuum conditions, the throwing objects are moving inside the barrel completely without frictions, and the velocity obtained is the maximum value of the detonation-driven velocity; (2) In value simulation, the length of barrel is certain, the air field is added in the model, the particle layers are scattered under function from the high pressure and the pressure inside the barrel is increased, their collisions with the barrel under function from the detonation products have reduced the velocity, the expansion waves at the port and the complicated flow field of the detonation products make the particle groups in an elongation and scattering state, with a big velocity gradient; (3) The front part of the barrel is short, as a result, the increase of particle velocity after increasing the explosive charge is not as large as the theoretical value.

TABLE 6: COMPARISONS BETWEEN SIMULATION RESULTS AND THEORETICAL ANALYSES

	Mass ratio of explosive /particle	Theoretical value (m/s)	Average velocity (m/s)	Maximum velocity of single particle (m/s)	Difference between theoretical value (m/2)	Percentage
1	0.5:1	802.62	435.83	782.63	19.99	2.5%
2	1:1	1337.31	768.61	1162.92	174.39	13.0%
3	2:1	2042.59	1007.51	1525.22	517.37	25.3%

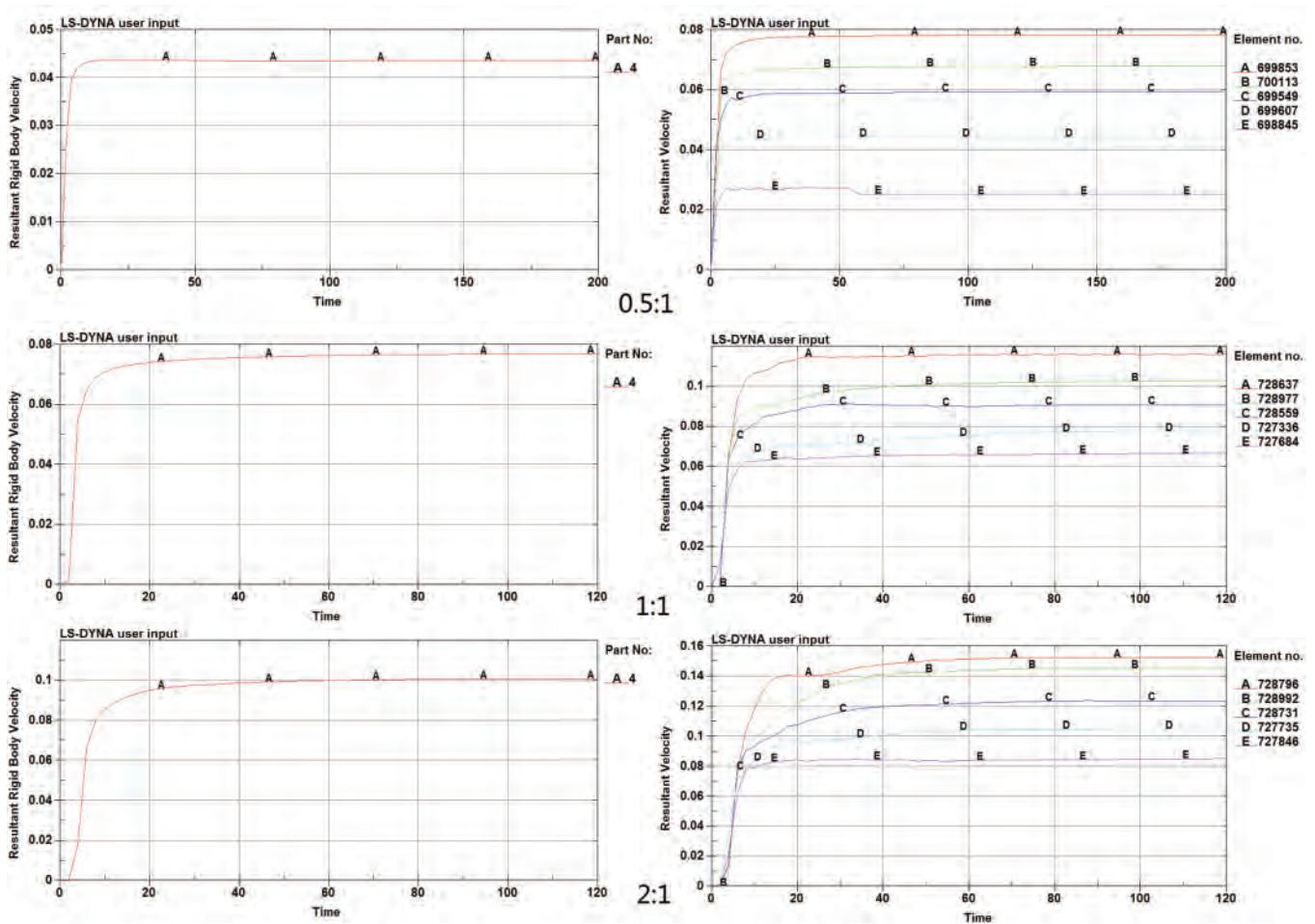


Fig.6 The overall average velocity of particle dispersing and single particle velocity process curve

4.4 DISPERSING OF PARTICLES

Fig.7 gives the particle group shape outlines after dispersing in three explosive/particle mass rates upon finishing the calculations.

The left side in Fig.7 is a front view, from which you could see the particle groups are in a elongated state, and they basically disperse alongside the axis, with even distribution and a good orientation; as for the computing duration for the 0.5 time explosive/particle mass ratio is long, so the tensile elongation is bigger than the latter; the right side in Fig.7 is a front view facing the heading direction of particles, the particle groups are distributed on the circle with diameter of 2 cm, the particles on circular surface in the middle of the circle are more dense, with the following reasons: the detonation products are reflected after dispersing toward the barrel wall and encountering the barrel, and gather at the central part (when $t=4\mu s$ in Fig.5), so that the particles in central part are pushed toward the barrel wall, while the collisions and rebounding between the particles and the barrel walls make the particles to gather toward the center, and finally the particles are gathered on the circular surface after repeating.

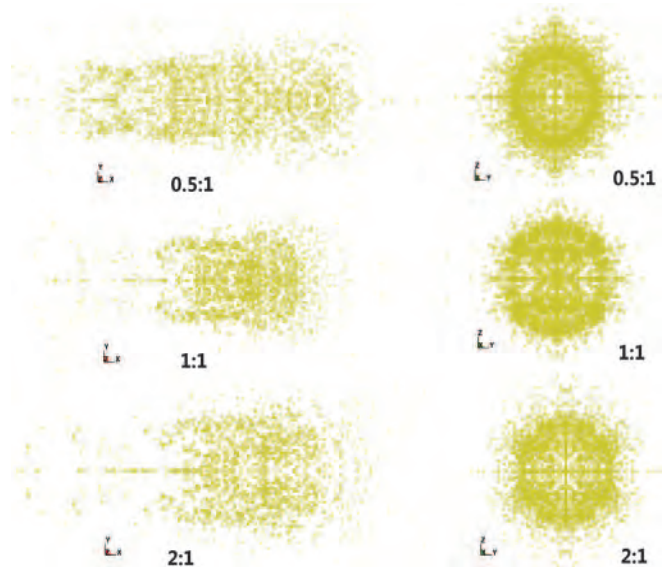


Fig.7 Particle group dispersing shape diagram

Continued on page 244